Photochemical & Photobiological Sciences

TECHNICAL NOTE

View Article Online
View Journal | View Issue

Cite this: *Photochem. Photobiol. Sci.*, 2016, **15**, 589

Construction of a multipurpose photochemical reactor with on-line spectrophotometric detection†

Tamás Ditrói,[a] József Kalmár,[b] Jose Angel Pino-Chamorro,[a] Zsolt Erdei,[a] Gábor Lente*[a] and István Fábián[a]

Received 31st October 2015,
Accepted 22nd February 2016

DOI: 10.1039/c5pp00407a

www.rsc.org/pps

A versatile photoreactor was built for studying homogeneous and heterogeneous photochemical reactions using fiber-optic devices. The reactor was designed to allow simultaneous photochemical initiation and online spectrophotometric monitoring of the reaction using independently controlled excitation and detection lamps. The system consists of a CCD spectrophotometer, a thermostated sample holder, two light sources, and standard 1.00 × 1.00 cm (or possibly smaller) fluorescence cuvettes, all coupled with fiber optic cables. The device can be used as a photoreactor, a diode-array spectrophotometer and also as a spectrofluorimeter. The reactor can be used in flow-through operation modes. Performance tests of the instrument are reported here with a number of known photochemical systems.

Introduction

The light sources of diode array spectrophotometers have high enough luminosity to initiate photochemical reactions during measurements, which is a major possible source for erroneous conclusions, but also makes this instrument a suitable tool for photochemical studies.[1–7] This technique can record high quality kinetic curves with very good time resolution, which are really necessary in modern chemical kinetics for drawing solid conclusions,[8] but also has some disadvantages as the light beam used to drive the photoreaction is the same as the analyzing light beam. Therefore, detection is impossible when the strong illumination beam is turned off, which may occasionally be a significant limitation in the case of photoinitiated chain mechanisms.[4,8] Another problem with this setup is that modifying the spectral characteristics of the driving light also influences the performance of spectrophotometric monitoring. Despite these disadvantages, using diode array spectrophotometers to study the kinetics of overall photochemical reactions seems to have considerable potential[1–7,9–11] especially because other kinetic techniques are usually limited to determine the lifetime of excited state species appearing as intermediates in such processes. Yet it is clear that decoupling the excitation and analyzing light beams could provide rather useful novel information.

Efforts to achieve this goal have already been reported by Gombár *et al.*, who used different LEDs as excitation light sources in a fiber-optic CCD spectrophotometer.[10] The LEDs were housed above the cuvette, which made the illumination path length dependent on the overall sample volume, therefore making volume-dependent studies, which often yield useful information,[2,7,10] difficult to carry out. Although there has been quite spectacular improvement in LED technology recently and LEDs are now available with a reasonably narrow spectral band width at a wide variety of wavelengths, the relatively low light intensity of these devices also poses a limit on the reported design.[10]

This work reports the construction of a photochemical reactor with a high intensity xenon lamp as an excitation light source and an independent fiber-optic CCD spectrophotometer as a detection tool. The geometry of the system allows for an additional method of monitoring, *e.g.* immersion of ion selective electrodes, and also facilitates a flow-through type operation mode. The possible uses of the newly developed instrument were demonstrated in known homogeneous and heterogeneous photoreactions.

Experimental

Materials

$Na_2S_2O_5$ of analytical grade was purchased from Reanal. $Ce_2(SO_4)_3$ (≥99.99% trace metals basis), methylene blue (reagent grade), 2,4,6-trichlorphenol, 2,6-dichloro-1,4-benzoquinone, 1,3-dihydro-1,3,3-trimethylspiro[2*H*-indole-2,3′-[3*H*]-naptho-2,1-*b*][1,4]oxazine], tris(2,2′ -bipyridyl)dichlororuthenium(II) hexahydrate and microcrystalline anatase (TiO_2,

[a]*Department of Inorganic and Analytical Chemistry, University of Debrecen, P.O.B. 21, Debrecen, H-4010 Hungary. E-mail: lenteg@science.unideb.hu*
[b]*MTA-DE Homogeneous Catalysis and Reaction Mechanisms Research Group, P.O.B. 21, Debrecen, H-4010 Hungary*

† Electronic supplementary information (ESI) available: Figures and images referred to in the text. See DOI: 10.1039/c5pp00407a

nanopowder, particle size <25 nm, specific surface area 45–55 $m^2\ g^{-1}$, melting point 1825 °C, density 3.9 g mL^{-1} at 25 °C, bulk density 0.04–0.06 g mL^{-1}) were all obtained from Sigma-Aldrich. $K_3[Fe(C_2O_4)_3]$ for the actinometric measurements was synthesized as described earlier.[11–13] Solutions were prepared using double distilled and Millipore-Q filtered water.

Instrument parts

All the parts of the reactor were purchased from Avantes including the detection light source (AvaLight-DHc), the light attenuator (Avantes ATT-INL, 0–100%), the fiber-optic switch, the spectrometer (Avaspec-2048L-TEC-RS) and the excitation lamp (AvaLight LDXE). The sample holder unit with a built-in magnetic stirrer was custom designed by Quantum Northwave. The softwares used to control the detection and the illumination system were Avasoft 7.5 and Matlab 7.10.0.499. The temperature and the rate of stirring were controlled with Q-blue software. In flow-through experiments, a Gilson Minipuls 2 peristaltic pump was used, which holds two tubes in tandem and has an adjustable rate between 1 and 25 rpm.

Results and discussion

Design of the photoreactor

The reactor was designed to enable the monitoring of a photoreaction spectrophotometrically while the sample is illuminated independently. Therefore, separate detection and excitation light sources were used as shown in Fig. 1 (photo shown as Fig. S1 in the ESI†). The excitation part of the system consists of the light source itself, an attenuator and a programmable fiber-optic switch before reaching the sample holder. The excitation lamp is an AvaLight LDXE xenon lamp with a 1000 nm laser focused on it, and emits intense light in a broad wavelength range (from 170 to 1100 nm, spectrum shown in Fig. S2 in the ESI†). This lamp has a stable intensity and an expected lifetime over 10 000 h.

The light from the lamp is guided into a simple attenuator with a silica-core fiber-optic cable. Using the attenuator aperture, the intensity of the excitation light can be decreased if the adjustment of the photon flux is necessary. Actinometry or a similar calibration is necessary (see later) to determine the degree of attenuation after every adjustment. The light is then guided into the fiber-optic switch, which can shut off the excitation light as needed using a manual switch on the device or through a TTL signal from the spectrometer with a maximum switching rate of 50 Hz. The programmable mode makes it possible to create illumination patterns in experiments as needed to extract valuable kinetic data.

The fiber-optic switch can also hold 5 mm thick rectangular optical filters. Using appropriate cut-off, cut-on or bandpass filters, the spectral properties of the excitation light can be tuned. The design of this fiber optic switch is such that it can also be used as a second, non-thermostated cell holder during flow-through experiments.

The sample holder is placed at the end of the excitation line and serves as the central unit of the system. It is a modified Qpod 2e temperature controlled cuvette holder (Quantum Northwave). The holder is equipped with a built-in Peltier-module to control the temperature and a built-in magnetic stirring unit (stirring rate adjustable in its software up to a maximum of 1000 rpm, typically with 6 mm Teflon stirring rods). The sample holder can house standard 1.00 × 1.00 cm (or smaller, possibly custom-made) four-sided fluorescence cuvettes. The holder has four ports on its four sides (Fig. 2) for connecting the appropriate optical components. The volume of the sample solution in this cell can be varied between 1.50 and 3.50 cm^3. This is a very advantageous feature of the new reactor as decreasing sample volumes during photochemical studies is often desirable.[14]

Out of the four ports, the two opposite ones are used for excitation while the other two are used for detection. One of these pairs is modified to allow for some vertical adjustment of the ports therefore enabling vertical separation of the plane of excitation and the plane of detection by a maximum of 6 mm (illustration in Fig. S3 of the ESI†). This setup eliminates the possibility of the excitation light entering the detection line by light scattering. When using fluorescent substances, the fluorescent light can be excluded from the detected signal by separating the two planes. If fluorimetric detection is used, the excitation and detection ports are set to identical heights. Three of the ports on the sample holder can accommodate collimating lenses, one may also house a flat faced mirror plug

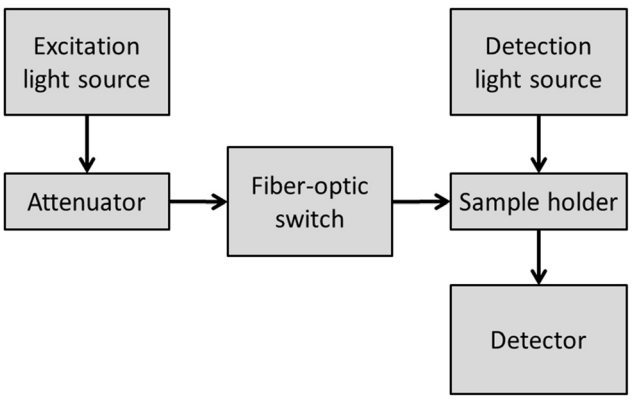

Fig. 1 General scheme of the photoreactor.

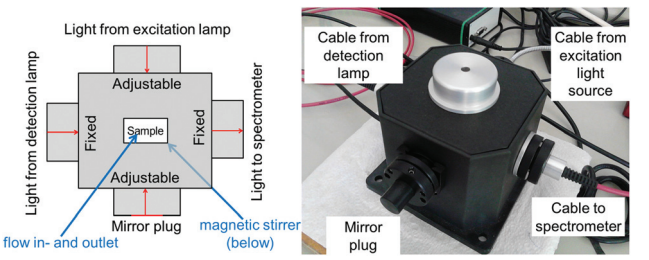

Fig. 2 Scheme and the photo of the sample holder.

after the sample opposite to the excitation port, which effectively doubles the excitation path length as illustrated in Fig. 2.

Using the built-in Peltier module, the temperature can be adjusted between −30 and +110 °C (an outer water reservoir is connected to cool the Peltier unit). Inert gas purging of the sample holder compartment is also possible through a port in order to avoid vapor condensation at low temperatures (below room temperature) or to facilitate measurements in the deep UV. Our tests were carried out between 5.0 and 60.0 °C.

The other key part of the setup is the on-line photometric monitoring system, which consists of a detection light source and a detector. The light source is a combined deuterium–halogen lamp with continuous emission from 200 to 2500 nm. Its intensity is more than ten thousand times lower than that of the excitation light source. Testing whether this very low light (detection) intensity influences the studied system is possible by closing the shutter of the excitation beam. The spectrometric detector (Avantes Avaspec 2048L-TEC-RS) is at the end of the detection line. This is a CCD detector containing 2048 thermo-electrically cooled pixels with a 300 line per mm grating for the wavelength range 170–1100 nm and has a special coating to increase UV-sensitivity and order-sorting filters to reduce second order effects. The spectral resolution and the sensitivity can be altered within certain limits by choosing a suitable slit. The minimum integration time is 1.3 ms, which compares quite favorably with commercial diode array spectrophotometers, where the typical minimum is 0.1 s.

Application modes of the instrument

In addition to its main use as a programmable photoreactor, our instrument has a number of other applications as well. To use it as a spectrophotometer, one only needs to shut off the excitation light. Compared to diode array spectrophotometers, the recording speed is high and the light intensity is low in a CCD instrument, which may be advantageous when light sensitive materials are studied. For fluorescence or phosphorescence studies, the excitation port on the sample holder is lowered to the same level as the detection ports, and the detection lamp is turned off. In this mode, the progress of a photochemical process can also be monitored if one of the involved components shows fluorescence. A mirror can also be placed into the detection light inlet to reflect the emitted light into the detection port and increase the fluorescence sensitivity. Phosphorescence lifetime measurements can be carried out by shutting off the excitation light after a brief initial period and recording the changes in the emission spectrum. The determination of turbidity is also possible in this setup by scattering at a 90° angle.

Performance tests

As the first performance test, the reaction between iodine and chlorate ions in acidic medium was used, which is understood to be a photoinitiated autocatalytic reaction.[4] A key point in the proposed mechanism is that light is only needed to produce some autocatalysts, but it is unnecessary when the autocatalytic pathway speeds up. In the earlier study, this point could be proved by an indirect experiment in which light was switched off after an initial period.[4] Using the present photoreactor, this crucial point could be demonstrated directly by switching off the excitation light before the end of the induction period. As expected (Fig. 3), the induction period was slightly longer, but the kinetic trace was very similar to the one detected under continuous illumination.

In the photoinitiated and cerium(III) catalyzed autoxidation of sulfur(IV),[9] a particularly interesting feature of the mechanism is that the loss of sulfur(IV) continues (albeit with a decreasing rate) for some time after the illumination is stopped. In the earlier study, indirect experimental evidence was obtained for this phenomenon from analyzing experiments done with the introduction of dark intervals of the gradually increasing length.[9] In the present reactor, direct evidence of this somewhat counterintuitive phenomenon could be obtained as shown in Fig. S4 and S5 in the ESI.†

A photochromic material, 1,3-dihydro-1,3,3-trimethylspiro[2*H*-indole-2,3′-[3*H*]naptho-2,1-*b*][1,4]oxazine] (PCR)[15–17] was found to be ideal for demonstrating the capabilities of the constructed photoreactor. A solution of this substance in ethanol was illuminated by switching on the excitation light beam. As shown in Fig. 4, the photochromic equilibrium was reached in less than 10 s. Discontinuing the illumination resulted in a switch back to the original form, and the change was again complete within 10 s. The high time resolution of the present photoreactor is essential here to study the kinetics of the interchange of the two forms.

Further tests with the known homogeneous aqueous photoreactions of 2,4,6-trichlorophenol (TCP)[18–20] and 2,6-dichloro-1,4-benzoquinone (DCQ)[2,21] were also carried out (see Fig. S6 and S7 in the ESI†). The aqueous photodegradation of TCP, which was reported to have a quantum yield of 0.02–0.03,[19] was driven to completion in about 120 min in the new photoreactor (Fig. S6 in the ESI†). The reported quantum yield of the photodegradation of DCQ is close to 1,[2,21] and the process was

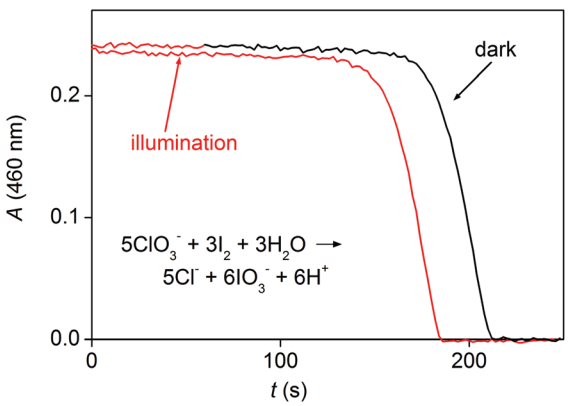

Fig. 3 Kinetic traces detected in the chlorate–iodine reaction. [I_2] = 0.38 mM, [ClO_3^-] = 25 mM; [$HClO_4$] = 1.0 M; path length: 1.00 cm; T = 25.0 °C; V = 3.00 cm^3; stirring: 800 rpm. Red curve: continuous illumination. Red-black curve: illumination switched off after 60 s.

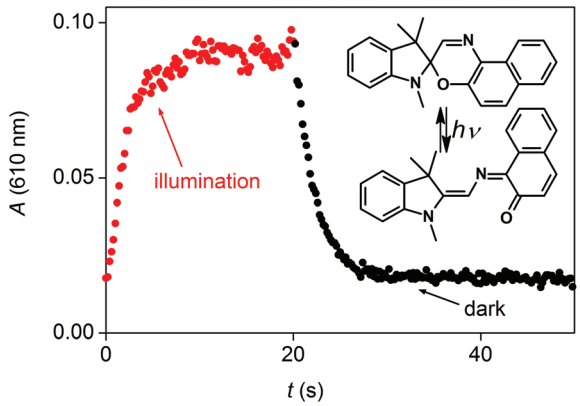

Fig. 4 Kinetic traces detected in a solution of the photochromic material 1,3-dihydro-1,3,3-trimethylspiro[2*H*-indole-2,3′-[3*H*]naptho-2,1-*b*][1,4]oxazine] (PCR). [PCR] = 8.92 mM (in ethanol); path length: 1.00 cm; T = 25.0 °C; V = 3.00 cm^3; stirring: 800 rpm.

completed in 5 min using the new photoreactor (Fig. S7 in the ESI†). In the earlier photochemical study using a diode array spectrophotometer, the reaction time was about 90 min.[2] These facts indicate that the xenon lamp used for excitation in our experimental setup has sufficient high intensity for applications even in the UV range.

To test the applicability of the reactor in heterogeneous systems, TiO_2 (anatase) was used in a few examples as a photocatalyst in the decomposition of organic materials. Fig. 5 shows an example where TCP was used as a test material to be degraded.[22,23] From this example, it is clear that the time resolution in these experiments was high enough to follow even the initial fast adsorption of TCP onto the surface of the solid photocatalyst as shown by a rapid initial absorbance decrease on the kinetic trace.

In similar experiments, the decomposition of methylene blue, another process with a considerable literature

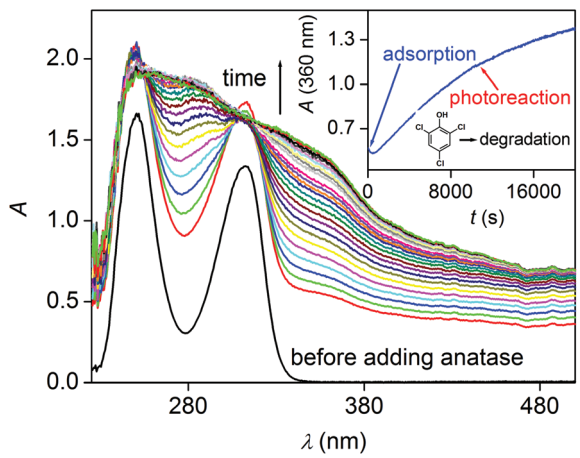

Fig. 5 Photochemical degradation of 2,4,6-trichlorophenol (TCP) in the presence of suspended anatase as a heterogeneous photocatalyst. [TCP] = 0.30 mM; $c(TiO_2)$ = 250 μg mL^{-1}; pH = 6.94 (75.0 mM phosphate buffer); path length: 1.00 cm; T = 25.0 °C; stirring: 1000 rpm.

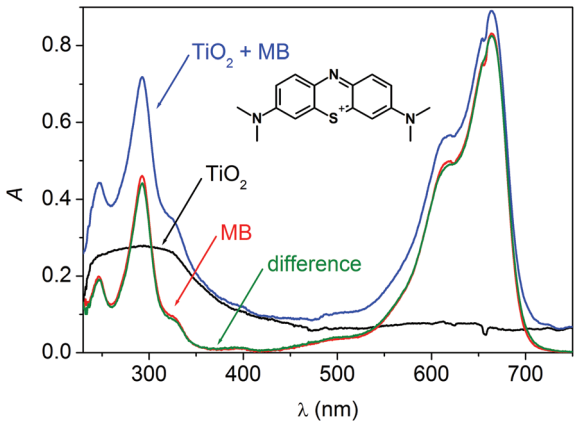

Fig. 6 Demonstration of the additivity of apparent absorbance values in the heterogeneous system containing anatase and methylene blue in the present photoreactor (stirring: 1000 rpm, path length: 1.00 cm). MB: homogeneous solution of methylene blue; TiO_2: suspension of anatase in water; TiO_2 + MB: suspension of anatase in a solution of methylene blue; difference: the difference of the spectra TiO_2 + MB and TiO_2.

background,[24–29] was also monitored in a heterogeneous system (Fig. S8†). An interesting and crucially important observation was made here. When dispersed solid particles are present in the solution, their light scattering contributes to the instrumentally measured absorbance despite the fact that it does not originate from absorption. This may cause difficulties in analyzing the data in a fully quantitative manner. In our photoreactor, the absorbance contributions coming from the light scattering and the absorption of the dissolved material seem to be additive if the stirring is intense enough (1000 rpm). This was proved by a series of experiments where the spectra of a homogeneous methylene blue solution, an anatase suspension and their mixture were recorded. As shown in Fig. 6, subtracting the spectrum of the anatase suspension from the spectrum of the mixture gave the exact spectrum of the homogeneous methylene blue solution. Therefore, the concentration of methylene blue can be calculated directly from the spectra based on Beer's law after an appropriate calibration (Fig. S9 in the ESI†), and on-line monitoring of the kinetics of the heterogeneous process is quite feasible. A similar experiment using a commercial diode array spectrophotometer failed to demonstrate a similar additivity (Fig. S10 in the ESI†), so this property seems unique to our experimental setup. The reason for this unexpected additivity in our photoreactor may be due to the presence of collimating lenses in the detection light beam.

Actinometry

The emission intensity of the lamp used to drive the photochemical processes in the new reactor can be advantageously determined by ferrioxalate actinometry.[12,13] Recently, Lehóczki *et al.* have reported an improvement of this method in which the concentration of iron(II) formed is calculated directly from the spectral changes of the actinometric solution rather than from a separate analysis step.[11] The improvement makes

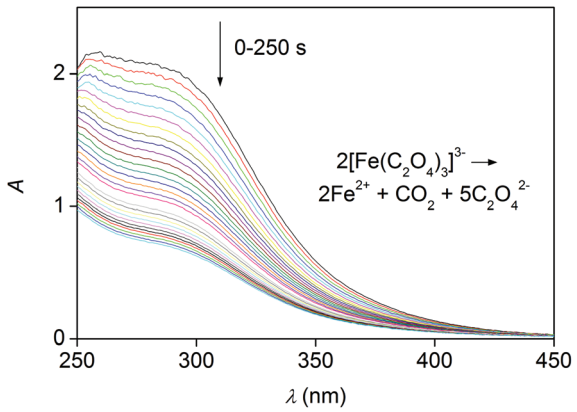

Fig. 7 Spectral changes in the actinometric solution during illumination. 15 mg of solid $K_3[Fe(C_2O_4)_3]$ was dissolved in 25 cm^3 of 0.050 M H_2SO_4 to prepare the actinometric solution, 2.50 cm^3 of which was irradiated for 250 s in the experiments shown (stirring: 1000 rpm, path length: 1.00 cm).

chemical actinometry faster and more robust without any loss in the precision of the results[11] and ideally suits the on-line monitoring built into the new photoreactor. Following the procedure described in the literature,[11] the total photon flux of the xenon lamp at the cuvette of the reactor was determined to be $(6.2 \pm 0.1) \times 10^{-8}$ mol s^{-1} (190–1100 nm range, the photochemical nomenclature used here adopts the latest recommendations of IUPAC[30]). The recorded spectral changes in the actinometric solution are displayed in Fig. 7, whereas a sample kinetic trace at 330 nm (which is ideal for the calculations[11]) is shown in Fig. S11 of the ESI.† The calculated intensity spectrum of the lamp is shown in Fig. S2 in the ESI,† as already mentioned.

Flow-through possibilities

Flow photochemistry is a currently emerging field.[14,31–33] The new photoreactor can also be operated in a flow-through mode using a peristaltic pump with two tubes in two different setups. The flow inlet and outlet are placed at the top of the four-sided fluorescence cuvette. Alternatively, a 1.00 cm flow-through cell is used in the sample holder for illumination and a second flow-through cell is placed into the fiber optic switch for detection (Fig. S12 in the ESI†). TCP degradation with and without the photosensitizer tris(2,2′-bipyridyl)ruthenium(II)[34,35] ion was used to test this operation mode (Fig. S13 in the ESI†).

Conclusions

The present work shows that a multifunctional modular photoreactor using on-line spectrophotometric detection of a very high time resolution can be readily constructed from commercially available parts with minimal modifications. The sample volume is small and easily controllable between 1.50 and 3.50 cm^3 with a single standard fluorimetric cuvette. The instrument can yield high-quality kinetic information on overall photochemical processes, both in homogeneous and heterogeneous systems. A recently developed on-line actinometric method can be used in this instrument very easily. This photoreactor may find versatile uses in the study of photochemical processes including flow-through systems.

Acknowledgements

The authors thank the Hungarian Science Foundation (NK 105156) and the University of Debrecen (RH/751/2015) for financial support. The research was supported by the EU and co-financed by the European Social Fund under the project ENVIKUT (TÁMOP-4.2.2.A-11/1/KONV-2012-0043). The assistance of Ms Hajnalka Csarnai and Mr André Spanhol is also acknowledged. An anonymous reviewer is also thanked for pointing out the importance of the flow-through operation mode.

Notes and references

1 D. M. Stanbury and J. N. Figlar, *Coord. Chem. Rev.*, 1999, **187**, 223–232.
2 G. Lente and J. H. Espenson, *J. Photochem. Photobiol., A*, 2004, **163**, 249–258.
3 D. Varga, A. K. Horváth and I. Nagypál, *J. Phys. Chem. B*, 2006, **110**, 2467–2470.
4 M. Galajda, G. Lente and I. Fábián, *J. Am. Chem. Soc.*, 2007, **129**, 7738–7739.
5 Á. Filáry and A. K. Horváth, *Phys. Chem. Chem. Phys.*, 2010, **12**, 6742–6749.
6 T. Zidki, H. Cohen and D. Meyerstein, *Phys. Chem. Chem. Phys.*, 2010, **12**, 12862–12867.
7 I. Fábián and G. Lente, *Pure Appl. Chem.*, 2010, **82**, 1957–1973.
8 J. H. Espenson, *Chemical Kinetics and Reaction Mechanisms*, McGraw-Hill, New York, 2nd edn, 1995.
9 I. Kerezsi, G. Lente and I. Fábián, *J. Am. Chem. Soc.*, 2005, **127**, 4785–4793.
10 M. Gombár, É. Józsa, M. Braun and K. Ősz, *Photochem. Photobiol. Sci.*, 2012, **11**, 1592–1595.
11 T. Lehóczki, É. Józsa and K. Ősz, *J. Photochem. Photobiol., A*, 2013, **251**, 63–68.
12 C. G. Hatchard and C. A. Parker, *Proc. R. Soc. London, Ser. A*, 1956, **235**, 518–536.
13 N. J. Bunce, in *CRC Handbook of Organic Photochemistry*, ed. J. C. Scaiano, CRC Press, Boca Raton, 1989, vol. 1, pp. 241–259.
14 E. E. Coylea and M. Oelgemöller, *Photochem. Photobiol. Sci.*, 2008, **7**, 1313–1322.
15 S. Schneider, A. Mindl, G. Elfinger and M. Melzig, *Ber. Bunsen-Ges.*, 1987, **91**, 1222–1224.
16 F. Maurel, J. Aubard, M. Rajzmann, R. Guglielmetti and A. Samat, *J. Chem. Soc., Perkin Trans. 2*, 2002, 1307–1315.

17 S. Nakamura, K. Uchida, A. Murakami and M. Irie, *J. Org. Chem.*, 1993, **58**, 5643–5545.
18 B. E. Sturgeon, B. J. Battenburg, B. J. Lyon and S. Franzen, *Chem. Res. Toxicol.*, 2011, **24**, 1862–1868.
19 F. J. Benítez, J. Beltrán-Heredia, J. L. Acero and F. J. Rubio, *Ind. Eng. Chem. Res.*, 1999, **38**, 1341–1349.
20 M. Hu, Y. Wang, Z. Xiong, D. Bi, Y. Zhang and Y. Xu, *Environ. Sci. Technol.*, 2012, **46**, 9005–9011.
21 H. Görner and C. von Sonntag, *J. Phys. Chem. A*, 2008, **112**, 10257–10263.
22 E. Pino and M. V. Encinas, *J. Photochem. Photobiol., A*, 2012, **242**, 20–27.
23 J. A. Rengifo-Herrera, R. A. Frenzel, M. N. Blanco and L. R. Pizzio, *J. Photochem. Photobiol., A*, 2014, **289**, 22–30.
24 X. Yan, T. Ohno, K. Nishijima, R. Abe and B. Ohtani, *Chem. Phys. Lett.*, 2006, **429**, 606–610.
25 M. Pudukudy, Z. Yaakob, R. Rajendran and T. Kandaramath, *React. Kinet., Mech. Catal.*, 2014, **112**, 527–542.
26 Y. Zhou, W. Hu, J. Yu and F. Jiao, *React. Kinet., Mech. Catal.*, 2015, **115**, 581–596.
27 N. K. Eswar, P. C. Ramamurthy and G. Madras, *Photochem. Photobiol. Sci.*, 2015, **14**, 1227–1237.
28 J. Kalmár, M. Kéri, Z. Erdei, I. Bányai, I. Lázár, G. Lente and I. Fábián, *RSC Adv.*, 2015, **5**, 107237–107246.
29 J. Kalmár, G. Lente and I. Fábián, *Dyes Pigm.*, 2016, **127**, 170–178.
30 S. E. Braslavsky, *Pure Appl. Chem.*, 2007, **79**, 293–465.
31 A. Yavorskyy, O. Shvydkiv, N. Hoffmann, K. Nolan and M. Oelgemöller, *Org. Lett.*, 2012, **14**, 4342–4345.
32 M. Oelgemöller, *Chem. Eng. Technol.*, 2012, **35**, 1144–1152.
33 S. Elgue, T. Aillet, K. Loubiere, A. Conté, O. Dechy-Cabaret, L. Prat, C. R. Horn, O. Lobet and S. Vallon, *Chem. Today*, 2015, **33**(5), 58–61.
34 A. Lewandowska-Andralojc and D. E. Polyansky, *J. Phys. Chem. A*, 2013, **117**, 10311–10319.
35 J. J. Stracke and R. G. Finke, *ACS Catal.*, 2014, **4**, 79–89.

